

Historical Trends of Atmospheric Black Carbon on Tibetan Plateau As Reconstructed from a 150-Year Lake Sediment Record

Zhiyuan Cong,^{†,||} Shichang Kang,^{†,‡,*} Shaopeng Gao,[†] Yulan Zhang,[†] Qing Li,^{†,§} and Kimitaka Kawamura^{||}

[†]Key Laboratory of Tibetan Environment Changes and Land Surface Processes, Institute of Tibetan Plateau Research, Chinese Academy of Sciences, Beijing 100101, China

[‡]State Key Laboratory of Cryospheric Sciences, Chinese Academy of Sciences, Lanzhou 730000, China

[§]Southwest University, Chongqing 400715, China

^{||}Institute of Low Temperature Science, Hokkaido University, Sapporo, 060-0819, Japan

S Supporting Information

ABSTRACT: Black carbon (BC) is one of the key components causing global warming. Especially on the Tibetan Plateau (TP), reconstructing BC's historical trend is essential for better understanding its anthropogenic impact. Here, we present results from high altitude lake sediments from the central TP. The results provide a unique history of BC over the past 150 years, from the preindustrial to the modern period. Although BC concentration levels in the Nam Co Lake sediments were lower than those from other high mountain lakes, the temporal trend of BC fluxes clearly showed a recent rise, reflecting increased emissions from anthropogenic activities. The BC records were relatively constant until 1900, then began to gradually increase, with a sharp rise beginning around 1960. Recent decades show about 2.5-fold increase of BC compared to the background level. The emission inventory in conjunction with air mass trajectories further demonstrates that BC in the Nam Co Lake region was most likely transported from South Asia. Rapid economic development in South Asia is expected to continue in the next decades; therefore, the influence of BC over the TP merits further investigations.



1. INTRODUCTION

Black carbon (BC) is the collective carbon-rich aromatic residues and condensates from the incomplete combustion of fossil fuels and biomass.¹ Given their small size (particularly with size less than 2.5 μm), these particles can remain airborne in the atmosphere for about one week, which is enough time to undergo long distance transport and reach even the most remote sites.² BC can absorb solar radiation, thereby warming the atmosphere, alter the albedo, accelerate glacier melting when deposited on snow, and change the properties (reflectivity and lifetime) of clouds as well as precipitation.^{3–5} The formation, transport, and deposition of BC also plays a significant role in the global carbon cycle.⁶

The Tibetan Plateau (TP) is the largest and highest plateau on earth, with an area of about 2 500 000 km^2 and an average elevation of more than 4000 m. The atmosphere over the TP is minimally disturbed by anthropogenic activities due to sparse population and limited industries. According to the earlier sunphotometer observations, very low annual aerosol optical depth (AOD) was recorded on the central TP.⁷ However, the TP is surrounded by regions with growing air pollution, especially in South and Southeast Asia.⁸ In some cases, widespread air pollution can enter the interior TP through atmospheric circulation.^{9,10} As the world's largest ice storage site after the Arctic and Antarctic, the glaciers on the TP are experiencing shrinkage particularly caused by increasing atmospheric BC deposition.^{11–13}

Understanding the temporal change of BC content in the atmosphere, especially its background burden before intensive industrialization, is crucial to assess the impact of human disturbance on atmospheric composition and thereafter climate change.¹⁴ However, the knowledge of its historical trend on the TP is very scarce.^{12,15,16} In addition to ice cores from alpine glaciers, lake sediments also serve as ideal archives for exploring climate and environment changes. There are more than 1500 lakes on the TP with sizes ranging from 0.01 to 4000 km^2 .¹⁷ In this study, we present results from Nam Co Lake sediments in the central TP, with the aim to investigate the temporal variability of BC deposition and reveal its links with emissions and transport.

2. MATERIALS AND METHODS

2.1. Sampling Site Description. Nam Co Lake, the second largest saline lake in China, is located on the central TP ($\text{N}30^{\circ}30' \sim 30^{\circ}56'$, $\text{E}90^{\circ}16' \sim 91^{\circ}03'$; 4722 m a.s.l.) (Figure S1, Supporting Information). Its area is 2015 km^2 , with the deepest water depth more than 90 m.¹⁸ According to the water chemistry survey, the pH and electric conductivity of the surface water are 9.21 and 1851 $\mu\text{S}\cdot\text{cm}^{-1}$, respectively,

Received: November 25, 2012

Revised: February 5, 2013

Accepted: February 12, 2013

Published: February 12, 2013

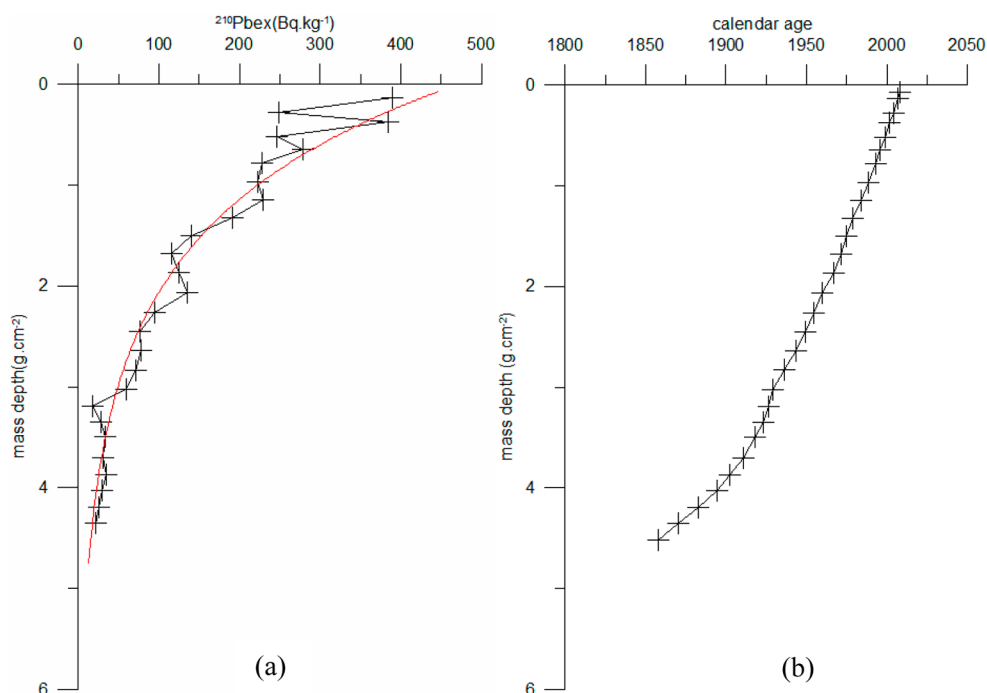


Figure 1. Sediment dating results. (a) Variations of $^{210}\text{Pb}_{\text{ex}}$ in NMC09 core; (b) depth versus age plot calculated by the CRS model.

Table 1. Averages of Black Carbon Concentrations ($\text{mg}\cdot\text{g}^{-1}$) and Deposition Fluxes ($\text{g}\cdot\text{m}^{-2}\cdot\text{a}^{-1}$) for This Study and Previous Work

lakes	description (altitude, m a.s.l)	age span	concn. (mean)	fluxes	methods
Nam Co	Tibetan Plateau, 4722 m	1857–2009	0.49–1.09 (0.74)	0.12–0.44 (0.26)	TOR-IMPROVE ^a
Daihai ³³	North China, 1221 m	1800–2001	0.52–4.90 (2.26)	0.6–7 (3.1)	TOR-IMPROVE
Taihu ³³	East China, 4 m	1825–2003	0.43–1.95 (1.01)	1.15–6.89 (3.29)	TOR-IMPROVE
West Pine Pond ³⁴	New York State, 484 m	1835–2005	0.6–8	0.026–0.77	TOT-STN ^b
Ledvica ³⁵	Alps, Slovenia, 1830 m	about 1815–1998	3.6–9.2	0.3–1.3	CTO-375 ^c
Engstlen ³²	Alps, Switzerland, 1850 m	1963–2008	1.5–3.3	2.1–7.4	CTO-375
Stora Frillingen ²⁴	Aspvreten, Sweden	1000s–2005		0.05–0.40	CTO-375

^aTOR-IMPROVE, thermal optical reflectance, following IMPROVE-A protocol. ^bTOT-STN, thermal optical transmittance, following STN protocol. ^cCTO-375, chemo-thermal oxidation at 375 °C.

indicating an alkaline and slightly brackish body of water. A more detailed description on the lake can be found in Wang et al.^{19,20} Because there is no outflow, the water balance of Nam Co Lake is controlled by the relationship among precipitation, inflow, and evaporation. The reason that Nam Co Lake was chosen for the BC historic variation research is due to its position within the interference zone of the Indian summer monsoon and the westerlies. Previous research has demonstrated that Nam Co Lake sediment could sensitively respond to the climatic and environmental changes.^{21–23}

In the Nam Co Lake region, annual precipitation is around 400 mm. Mean annual air pressure and temperature are 571.2 hPa and -0.4 °C, respectively. Mean annual relative humidity is 52.6%, and mean annual wind speed is 3.99 m \cdot s $^{-1}$. Surrounding Nam Co Lake is alpine steppe and meadow. Scarcely any atmospheric pollutant emission is in the vicinity due to its harsh environment and remoteness.⁷

2.2. Sediment Collection and Dating. In 2009, a sediment core (20 cm long, hereafter NMC09) was collected from the eastern basin of Nam Co Lake using a gravity coring system with a 6 cm diameter polycarbonate tube (Figure S1, Supporting Information). The water depth of the sampling site is 60 m. The core was sliced in the field at intervals of 0.5 cm,

stored in plastic bags, and kept frozen until analysis. The sediment chronology was constructed by measuring radio-nuclide (^{210}Pb) using γ -ray spectrometry (HPGe, ORTEC-GWL).

2.3. Sediment Pretreatment and BC Determination. Determination of BC in lake sediments is difficult due to its complex organic and mineral matrices. Several procedures for separating and determining BC from sediments have been developed.^{1,24–28} In the present work, the methods of Han et al.²⁵ were adapted. Briefly, the sediment samples were acid treated to avoid interference of minerals and then filtered using quartz filters with even distribution. The quartz filters were analyzed for BC using a DRI model 2001 carbon analyzer (Atmoslytic Inc., Calabasas, CA) following the IMPROVE-A protocol.²⁹ Detailed procedures for the sediment preparation and analytical method are summarized in the Supporting Information text. For quality control, standard reference material (marine sediment, NIST SRM-1941b) was also analyzed through the same procedure as for the NMC09 samples. Our BC values compare well ($97.6 \pm 2.2\%$, $n = 8$) to the values reported previously,³⁰ which indicates the analytical method used is reliable and repeatable. It should be noted that lake sediments determined by different methods such as

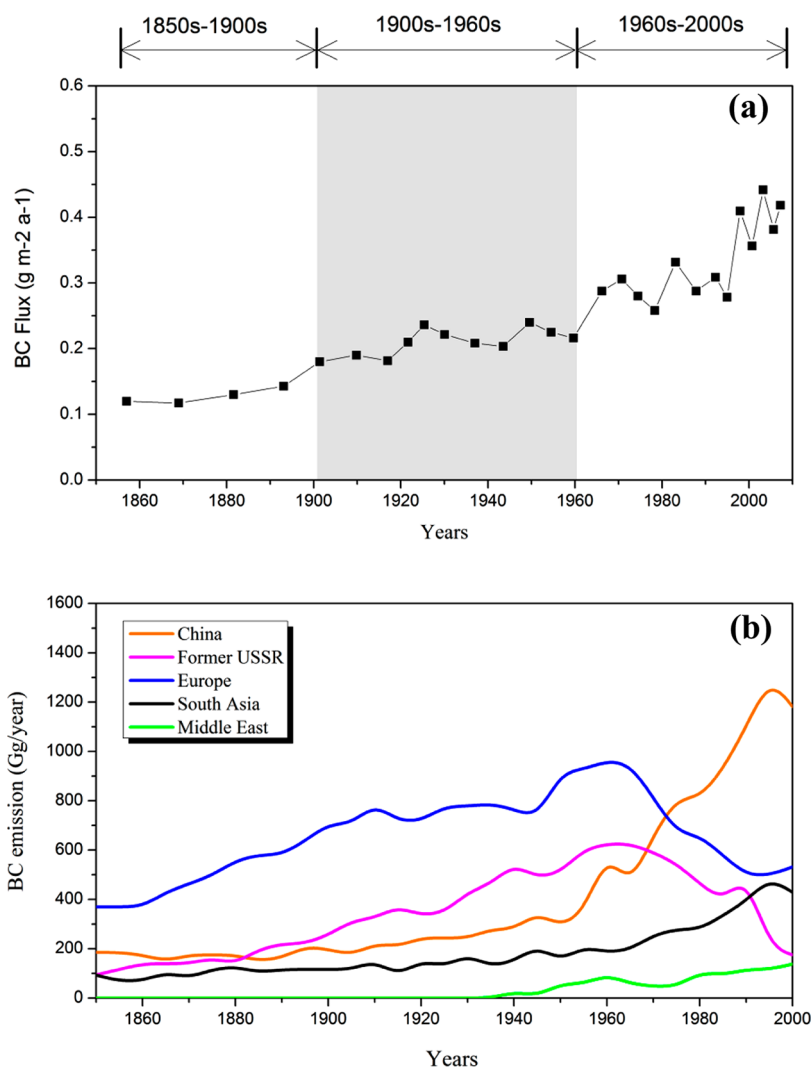


Figure 2. Variation of BC fluxes from 1857 to 2009 at Nam Co Lake (a) and BC historical emission data (b).³⁸

IMPROVE-A thermal optical reflectance (TOR), STN-thermal optical transmittance (TOT), and chemothermal oxidation (CTO) may produce different concentrations. For example, Han et al.²⁵ demonstrates that TOR methods could result in 10% higher black carbon than that from TOT method, while the BC value from CTO method is much lower, accounting for $1/7$ of that from TOR.

3. RESULTS AND DISCUSSION

3.1. Sediment Chronology. For NMC09, ages and sedimentation rates were calculated using the CRS (constant rate of supply) dating model.³¹ The sediment record covers about 150 years, reaching back to 1857 AD (Figure 1). The reliability of the core dating was acceptable based on a constant decline in ²¹⁰Pb with increasing depth. The sedimentation rate in this work ($1.2 \text{ mm}\cdot\text{a}^{-1}$) is consistent with previously reported value ($1.15 \text{ mm}\cdot\text{a}^{-1}$) by Wrozyzna et al.²¹ at the same lake.

3.2. Concentrations of BC in Sediments. BC concentrations in NMC09 varied from 0.49 to 1.09 with an average of $0.74 \text{ mg}\cdot\text{g}^{-1}$, much lower than those reported elsewhere^{32–35} (Table 1). For example, BC values in lake sediment cores from Daihai in North China and Taihu in East China ranged from 0.52 to $4.9 \text{ mg}\cdot\text{g}^{-1}$, and 0.43 to $1.95 \text{ mg}\cdot\text{g}^{-1}$, respectively.³³ The

higher BC levels may likely be due to intensive biomass burning and fossil fuel combustion in northern and eastern China. Husain et al.³⁴ reported BC concentrations varying from 0.6 to $8 \text{ mg}\cdot\text{g}^{-1}$ in a sediment core from Lake West Pine Pond, New York, over the past 170 years. Muri et al.³⁵ determined that BC concentrations in five high altitude alpine lake sediments in Slovenia ranged from 1 to $11 \text{ mg}\cdot\text{g}^{-1}$. The lower BC concentrations in Nam Co Lake sediments are clearly associated with the geographic characteristics of the TP, namely, its remote location, high altitude, and relatively pristine atmosphere. It should also be noted that different pretreatment procedures, analytical instruments, and protocols may produce noticeable discrepancies in BC results.¹ In addition, annual mean atmospheric BC concentration in the Nam Co Lake area was $82 \text{ ng}\cdot\text{m}^{-3}$, as determined in the previous work.³⁶ The corresponding BC concentration in the top section of the lake sediment core is $1.09 \text{ mg}\cdot\text{g}^{-1}$. Therefore, the ratio of BC concentration between the atmosphere and sediment can be roughly estimated to reconstruct the atmospheric BC loading in the past.

3.3. BC Deposition Flux and Its Historical Trends. Because BC concentration may be strongly affected by the dilution of detrital matter and water contents, deposition fluxes are better to reflect the real variation of BC input.^{24,34}

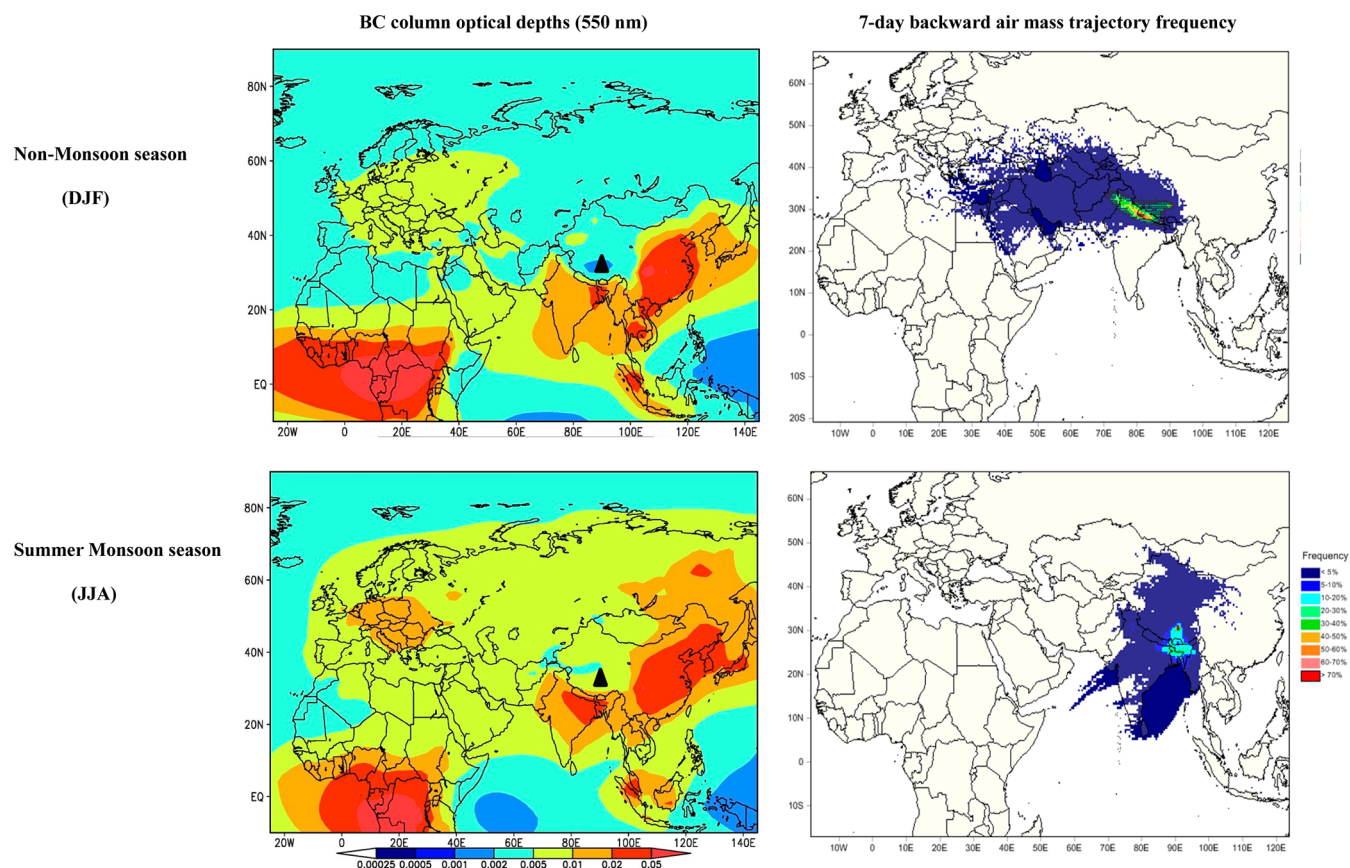


Figure 3. Average BC column optical depth (550 nm, GOCART model) during nonmonsoon and summer monsoon seasons from 2000 to 2007 (left) and the corresponding air mass trajectory frequency during this period (right). The location of Nam Co Lake is marked as a black triangle.

BC fluxes of Nam Co Lake sediments ranged from 0.12 to 0.44 $\text{g}\cdot\text{m}^{-2}\cdot\text{a}^{-1}$, with an average of 0.26 $\text{g}\cdot\text{m}^{-2}\cdot\text{a}^{-1}$. These values are about 10% of those in other Chinese lakes (i.e., Daihai and Taihu) and are also significantly lower than those from European high altitude lakes (Lake Engstlen and Lake Ledvica) and a North American mountain lake (West Pine Pond) (Table 1). Elmquist et al.²⁴ reported BC fluxes of 0.05–0.40 $\text{g}\cdot\text{m}^{-2}\cdot\text{a}^{-1}$ in sediments from Stora Frillingen Lake, Sweden, which appear comparable to those from Nam Co Lake. However, considering that the BC value from CTO methods is only $1/7$ of that from TOR, BC deposition at Nam Co Lake should be much lower than that from Stora Frillingen Lake.

Figure 2a shows the temporal trend of BC fluxes. From the 1850s to the early 1900s, fluxes are generally constant, which can be considered as background level without significant disturbance from human activities. After the 1900s, BC fluxes show a gradual and continuous increase, indicating that the influence from anthropogenic sources began in the interior TP. From the 1960s to the early 2000s, the increasing trend of BC flux accelerated significantly. Average BC flux for 1850s–1900s, 1900s–1960s, and 1960s–2009 was $0.13 \pm 0.01 \text{ g}\cdot\text{m}^{-2}\cdot\text{a}^{-1}$, $0.21 \pm 0.02 \text{ g}\cdot\text{m}^{-2}\cdot\text{a}^{-1}$, and $0.33 \pm 0.06 \text{ g}\cdot\text{m}^{-2}\cdot\text{a}^{-1}$, respectively. This means that the BC burden has increased by 2.5-fold from the background period to industrial times. Our profile is generally in agreement with the results from the Mt. Everest ice core, in which the BC concentrations have increased almost 3-fold from 1975 to 2000 when compared to the period 1860–1975.¹⁵ In the recent Atmospheric Chemistry and Climate Model Intercomparison Project,³⁷ historic BC aerosols were simulated by eight models, which were based mainly on 12 ice

core records from Greenland, the Antarctic, the TP, and the Alps. Interestingly, all of the models showed an increased global BC burden from the preindustrial to the present of 2.5–3 times, which matches well the BC temporal profile in Nam Co Lake.

Bond et al.³⁸ reconstructed a BC emission inventory for the past 150 years (1850–2000) for different regions of the world (Figure 2b). The increased profile of BC in Nam Co Lake sediment closely follows BC emission patterns of South Asia, China, and the Middle East, which all demonstrated a sharp increase beginning around 1950.

According to trace metals data from NMC09, typical anthropogenic heavy metals such as Pb and Zn all exhibit rapid increase since the 1960s (Figure S2, Supporting Information). Yang et al.²² determined the mercury history based on nine lakes from different regions of the TP. According to their results, a dramatic increase of Hg in Nam Co Lake sediments since the 1960s has also been found. The increase of BC in the last few decades is synchronous with the anthropogenic heavy metals, reconfirming that since the 1960s, the influence of anthropogenic pollutants on the TP has become more evident.

3.4. Potential Source Region of BC. Because there are few local emission sources in the Nam Co Lake region and even on the entire TP, BC is most likely transported over long distances from the surrounding areas of the TP by the action of air mass movement. Figure 3 shows the distribution of BC column optical depths at 550 nm (Jan. 1, 2000 to Dec. 31, 2007), which were produced by the GOCART model simulation.³⁹ The GOCART model uses the assimilated

meteorological fields of the Goddard Earth Observing System Data Assimilation System (GEOS DAS). The model has a horizontal resolution of 2° latitude by 2.5° longitude and 20–55 vertical sigma layers.⁴⁰ Our black carbon optical depth distribution pattern (Figure 3, left) is generally consistent with that simulated by the AeroCom median model.⁴¹ Figure 3 clearly shows that atmospheric BC widely exists in Africa, East China, and South and Southeast Asia with some seasonal variation.

To reveal the transport pathway of atmospheric BC to Nam Co Lake, backward trajectory analysis was conducted corresponding to BC column optical depth simulation (Jan. 1, 2000 to Dec. 31, 2007) using the HYSPLIT model and NCEP/NCAR reanalysis data.⁴² Seven-day (the typical atmospheric residence time of BC) backward trajectories were run at 500 m height above ground level for every 6 h daily. Furthermore, the trajectory frequency at each grid ($1^\circ \times 1^\circ$) was calculated using Trajstat software.⁴³ The backward trajectory results (Figure 3, right) reveal two distinct types of atmospheric circulation, corresponding to the Tibetan monsoon regime. In the summer monsoon season (June–August), air masses from Northeast India, Bangladesh, and the Bay of Bengal bring warm and moist air originating from the Indian Ocean. In the nonmonsoon season, strong westerly winds pass through the southern Himalayas (West Nepal, Northwest India, and Pakistan). According to the BC distribution (Figure 3, left) and previous research,^{44–46} high concentrations of atmospheric BC exist over the southern slope of Himalayas, the Indo-Gangetic plains, and Indian Ocean. Although the Himalayas are considered as a barrier to atmospheric pollution, previous research has demonstrated that high Himalayan valleys can act as a direct channel, capable of transporting air pollutants up to 5000 m a.s.l.,⁴⁷ and those pollutants could successively be transported trans-Himalayan and advected onto the TP.⁴⁸ Even ice cores from extremely high elevation of the Himalayas (e.g., East Rongbuk Glacier, Mt. Everest, 6518 m) exhibit an increasing influence of BC emissions from South Asia.¹⁵ Recently, we distinguished an intense spring pollution episode on 29th April 2009 in the Nam Co region.¹⁰ This episode was characterized by dominant fine particles with strong absorption, underlining the influence of biomass burning from South Asia.

Therefore, according to the backward trajectory, regardless of the shift of wind flow direction between summer monsoon and nonmonsoon seasons (Figure 3), the atmospheric BC that exists in South Asia can be transported to the Nam Co Lake region and thereafter deposited in the lake and settle down in the lake sediments. As shown in Section 3.3, the historical profile of BC deposition in the Nam Co Lake sediments coincides with the BC emission inventory data of South Asia. Namely, BC emissions grew rapidly in the latter half of the twentieth century, owing to population growth and increased combustion of coal, biofuel, and petroleum products.³⁸ The conclusion that the majority of BC over the TP is coming from South Asia is also consistent with other studies.⁴⁹ For example, Lu et al.⁴⁹ pointed out that the contribution of BC from South Asia may account for 67% of BC transported to the Himalayas and TP region (HTP) on an annual basis. Similarly, using the GEOS-Chem model, Kopacz et al.⁵⁰ found that South Asia is the main source region in all seasons for BC deposited on TP glaciers. However, they also proposed that the intensive BC emission in the eastern part of China (e.g., Sichuan Basin) could impose some influence on the HTP in summer.^{49,50} However, our trajectory result for the Nam Co region does not

support this hypothesis. Given the prevailing winds in both seasons (Figure 3), few air masses arriving at Nam Co Lake come from the east. The high loading of BC in eastern China does not likely impact the Nam Co region due to its downwind location to TP, despite the fact that it could be transported further east over the western North Pacific by westerlies. In addition, it appears that the Mediterranean, Middle East, and Central Asia regions are not major source regions of BC in Nam Co Lake region, because of the low level of BC and/or few backward trajectories passing through there (Figure 3).

3.5. Indication of BC_{LT-TOR} and BC_{HT-TOR} . Based on the temperature protocol in the analytical procedures, BC could be further divided into two fractions (BC_{LT-TOR} and BC_{HT-TOR}). BC_{LT-TOR} means the black carbon liberated at 580°C (LT, low temperature) in a He/O₂ condition minus the pyrolyzed carbon fraction, while BC_{HT-TOR} is defined as the sum of black carbon liberated at 740°C and 840°C (HT, high temperature). The ratio between BC_{LT-TOR} and BC_{HT-TOR} may provide useful information for the source interpretation.^{51,52} BC_{LT-TOR} represents the combustion debris from biomass and fossil fuel and retains some original structural information of the source material, while BC_{HT-TOR} is formed through the condensation of gas emitted from combustion process.

In the Nam Co Lake sediments, the BC concentrations are positively correlated with those of BC_{LT-TOR} ($R^2 = 0.78$). The BC_{LT-TOR} to BC_{HT-TOR} ratios varied from 3.19 to 6.30, with a mean value of 4.69, indicating that BC_{LT-TOR} is a predominant constituent of BC. This shows that biomass burning is the major contributor to BC in Nam Co Lake sediments. This finding is consistent with recent radiocarbon measurements from India that indicate the major fraction of BC emissions was produced by biomass combustions such as residential cooking and agricultural burning.⁵³ Interestingly, we found that the BC_{LT-TOR} to BC_{HT-TOR} ratios in NMC09 decrease continuously (Figure 4). According to previous research, the BC_{LT-TOR} to BC_{HT-TOR} ratios from biomass burning are much higher than those from coal combustion and vehicle exhaust.⁵⁴ Therefore, the gradual decrease in the BC_{LT-TOR} to BC_{HT-TOR} ratios toward the 21 century in the Nam Co Lake sediments reflects the changing contribution of fossil fuel combustion and biomass burning to BC. Since BC_{HT-TOR} has greater light-absorbing

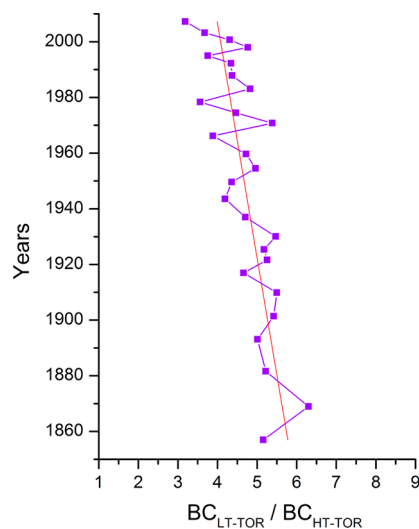


Figure 4. Ratios between BC_{LT-TOR} and BC_{HT-TOR} in Nam Co Lake sediments.

capacity than $BC_{LT-TOR}^{55,56}$ it merits more attention in terms of radiative forcing on the TP.

Rapid development of the South Asian economy is expected to continue in the next decades; thus, BC emissions from energy usage will increase continuously,⁵⁷ which will put further pressure on radiative forcing (warming) over the TP, especially on its alpine glaciers, under this scenario.

■ ASSOCIATED CONTENT

● Supporting Information

Detailed procedures for the sediment preparation and analytical method. This material is available free of charge via the Internet at <http://pubs.acs.org>.

■ AUTHOR INFORMATION

Corresponding Author

*Tel/Fax: 0086-10-84097092. E-mail: Shichang.kang@itpcas.ac.cn.

Notes

The authors declare no competing financial interest.

■ ACKNOWLEDGMENTS

This work was supported by the National Natural Science Foundation of China (41075089, 40830743, and 41001113) and the K. C. Wong Education Foundation. Special thanks to Dr. Wang Junbo for kindly providing the lake water depth map. The authors are grateful to Dr. Dong Shuping for his help in the BC analysis, Dr. Huang Jie for the sediment coring, and Dr. Betsy Armstrong for the English language editing.

■ REFERENCES

- (1) Hammes, K.; Schmidt, M. W. I.; Smernik, R. J.; Currie, L. A.; Ball, W. P.; Nguyen, T. H.; Louchouart, P.; Houel, S.; Gustafsson, O.; Elmquist, M.; Cornelissen, G.; Skjemstad, J. O.; Masiello, C. A.; Song, J.; Peng, P. a.; Mitra, S.; Dunn, J. C.; Hatcher, P. G.; Hockaday, W. C.; Smith, D. M.; Hartkopf-Froeder, C.; Boehmer, A.; Lueer, B.; Huebert, B. J.; Amelung, W.; Brodowski, S.; Huang, L.; Zhang, W.; Gschwend, P. M.; Flores-Cervantes, D. X.; largeau, C.; Rouzaud, J.-N.; Rumpel, C.; Guggenberger, G.; Kaiser, K.; Rodionov, A.; Gonzalez-Vila, F. J.; Gonzalez-Perez, J. A.; de la Rosa, J. M.; Manning, D. A. C.; Lopez-Capel, E.; Ding, L. Comparison of quantification methods to measure fire-derived (black/elemental) carbon in soils and sediments using reference materials from soil, water, sediment and the atmosphere. *Global Biogeochem. Cycles* **2007**, *21* (3), DOI: 10.1029/2006GB002914.
- (2) Masiello, C.; Druffel, E. Black carbon in deep-sea sediments. *Science* **1998**, *280* (5371), 1911–1913.
- (3) Hansen, J.; Nazarenko, L. Soot climate forcing via snow and ice albedos. *Proc. Natl. Acad. Sci. U.S.A.* **2004**, *101* (2), 423–428.
- (4) Flanner, M. G.; Zender, C. S.; Randerson, J. T.; Rasch, P. J. Present-day climate forcing and response from black carbon in snow. *J. Geophys. Res.—Atmos.* **2007**, *112* (D11), DOI: 10.1029/2006JD008003.
- (5) Andreae, M. O.; Jones, C. D.; Cox, P. M. Strong present-day aerosol cooling implies a hot future. *Nature* **2005**, *435* (7046), 1187–1190.
- (6) Gustafsson, Ö.; Gschwend, P. M. The flux of black carbon to surface sediments on the New England continental shelf. *Geochim. Cosmochim. Acta* **1998**, *62* (3), 465–472.
- (7) Cong, Z.; Kang, S.; Smirnov, A.; Holben, B. Aerosol optical properties at Nam Co, a remote site in central Tibetan Plateau. *Atmos. Res.* **2009**, *92* (1), 42–48.
- (8) Lelieveld, J.; Crutzen, P. J.; Ramanathan, V.; Andreae, M. O.; Brenninkmeijer, C. A. M.; Campos, T.; Cass, G. R.; Dickerson, R. R.; Fischer, H.; de Gouw, J. A.; Hansel, A.; Jefferson, A.; Kley, D.; de Laat,

A. T. J.; Lal, S.; Lawrence, M. G.; Lobert, J. M.; Mayol-Bracero, O. L.; Mitra, A. P.; Novakov, T.; Oltmans, S. J.; Prather, K. A.; Reiner, T.; Rodhe, H.; Scheeren, H. A.; Sikka, D.; Williams, J. The Indian Ocean Experiment: Widespread air pollution from South and Southeast Asia. *Science* **2001**, *291* (5506), 1031–1036.

(9) Wang, X.; Gong, P.; Yao, T.; Jones, K. C. Passive air sampling of organochlorine pesticides, polychlorinated biphenyls, and polybrominated diphenyl ethers across the Tibetan Plateau. *Environ. Sci. Technol.* **2010**, *44* (8), 2988–2993.

(10) Xia, X.; Zong, X.; Cong, Z.; Chen, H.; Kang, S.; Wang, P. Baseline continental aerosol over the central Tibetan plateau and a case study of aerosol transport from South Asia. *Atmos. Environ.* **2011**, *45* (39), 7370–7378.

(11) Ramanathan, V.; Carmichael, G. Global and regional climate changes due to black carbon. *Nature Geoscience* **2008**, *1*, 221–227.

(12) Xu, B.; Cao, J.; Hansen, J.; Yao, T.; Joswia, D. R.; Wang, N.; Wu, G.; Wang, M.; Zhao, H.; Yang, W.; Liu, X.; He, J. Black soot and the survival of Tibetan glaciers. *Proc. Natl. Acad. Sci. U.S.A.* **2009**, *106* (52), 22114–22118.

(13) Yasunari, T.; Bonasoni, P.; Laj, P.; Fujita, K.; Vuillermoz, E.; Marinoni, A.; Cristofanelli, P.; Duchi, R.; Tartari, G.; Lau, K. M. Estimated impact of black carbon deposition during pre-monsoon season from Nepal Climate Observatory–Pyramid data and snow albedo changes over Himalayan glaciers. *Atmos. Chem. Phys.* **2010**, *10*, 6603–6615.

(14) Andreae, M. O. Aerosols before pollution. *Science* **2007**, *315* (5808), 50–51.

(15) Kaspari, S.; Schwikowski, M.; Gysel, M.; Flanner, M.; Kang, S.; Hou, S.; Mayewski, P. Recent increase in black carbon concentrations from a Mt. Everest ice core spanning 1860–2000 AD. *Geophys. Res. Lett.* **2011**, *38*, L04703 DOI: 10.1029/2010GL046096.

(16) Ming, J.; Cachier, H.; Xiao, C.; Qin, D.; Kang, S.; Hou, S.; Xu, J. Black carbon record based on a shallow Himalayan ice core and its climatic implications. *Atmos. Chem. Phys.* **2008**, *8* (5), 1343–1352.

(17) Wang, S. M.; Dou, H. S. *Chinese Lakes Inventory*; Science Press: Beijing, China, 1998; p 580.

(18) Zhu, L.; Wu, Y.; Wang, J.; Lin, X.; Ju, J.; Xie, M.; Li, M.; Maeusbacher, R.; Schwalb, A.; Daut, G. Environmental changes since 8.4 ka reflected in the lacustrine core sediments from Nam Co, central Tibetan Plateau, China. *Holocene* **2008**, *18* (5), 831–839.

(19) Wang, J.; Zhu, L.; Daut, G.; Ju, J.; Lin, X.; Wang, Y.; Zhen, X. Investigation of bathymetry and water quality of Lake Nam Co, the largest lake on the central Tibetan Plateau, China. *Limnology* **2009**, *10* (2), 149–158.

(20) Wang, J.; Zhu, L.; Wang, Y.; Ju, J.; Xie, M.; Daut, G. Comparisons between the chemical compositions of lake water, inflowing river water, and lake sediment in Nam Co, central Tibetan Plateau, China, and their controlling mechanisms. *J. Great Lakes Res.* **2010**, *36* (4), 587–595.

(21) Wroczynna, C.; Frenzel, P.; Steeb, P.; Zhu, L.; van Geldern, R.; Mackensen, A.; Schwalb, A. Stable isotope and ostracode species assemblage evidence for lake level changes of Nam Co, southern Tibet, during the past 600 years. *Quat. Int.* **2010**, *212* (1), 2–13.

(22) Yang, H.; Battarbee, R. W.; Turner, S. D.; Rose, N. L.; Derwent, R. G.; Wu, G.; Yang, R. Historical reconstruction of mercury pollution across the Tibetan Plateau using lake sediments. *Environ. Sci. Technol.* **2010**, *44* (8), 2918–2924.

(23) Zhu, L. P.; Wu, Y. H.; Wang, J. B.; Lin, X.; Ju, J. T.; Xie, M. P.; Li, M. H.; Maeusbacher, R.; Schwalb, A.; Daut, G. Environmental changes since 8.4 ka reflected in the lacustrine core sediments from Nam Co, central Tibetan Plateau, China. *Holocene* **2008**, *18* (5), 831–839.

(24) Elmquist, M.; Zencak, Z.; Gustafsson, O. A 700 year sediment record of black carbon and polycyclic aromatic hydrocarbons near the EMEP air monitoring station in Aspveten, Sweden. *Environ. Sci. Technol.* **2007**, *41* (20), 6926–6932.

(25) Han, Y. M.; Cao, J. J.; Yan, B. Z.; Kenna, T. C.; Jin, Z. D.; Cheng, Y.; Chow, J. C.; An, Z. S. Comparison of elemental carbon in lake sediments measured by three different methods and 150-year

pollution history in Eastern China. *Environ. Sci. Technol.* **2011**, *45* (12), 5287–5293.

(26) Khan, A. J.; Swami, K.; Ahmed, T.; Bari, A.; Shareef, A.; Husain, L. Determination of Elemental Carbon in Lake Sediments Using a Thermal-Optical Transmittance (TOT) Method. *Atmos. Environ.* **2009**, *43* (38), 5989–5995.

(27) Schmidt, M. W. I.; Skjemstad, J. O.; Czimczik, C. I.; Glaser, B.; Prentice, K. M.; Gelin, Y.; Kuhlbusch, T. A. J. Comparative analysis of black carbon in soils. *Global Biogeochemical Cycles* **2001**, *15* (1), 163–168.

(28) Louchouart, P.; Chillrud, S. N.; Houel, S.; Yan, B.; Chaky, D.; Rumpel, C.; Largeau, C.; Bardoux, G.; Walsh, D.; Bopp, R. F. Elemental and molecular evidence of soot- and char-derived black carbon inputs to New York City's atmosphere during the 20th century. *Environ. Sci. Technol.* **2007**, *41* (1), 82–87.

(29) Chow, J. C.; Watson, J. G.; Chen, L. W. A.; Chang, M. C. O.; Robinson, N. F.; Trimble, D.; Kohl, S. The IMPROVE-A temperature protocol for thermal/optical carbon analysis: Maintaining consistency with a long-term database. *J. Air Waste Manage. Assoc.* **2007**, *57* (9), 1014–1023.

(30) Han, Y.; Cao, J.; An, Z.; Chow, J. C.; Watson, J. G.; Jin, Z.; Fung, K.; Liu, S. Evaluation of the thermal/optical reflectance method for quantification of elemental carbon in sediments. *Chemosphere* **2007**, *69* (4), 526–533.

(31) Appleby, P. G.; Oldfield, F. The calculation of lead-210 dates assuming a constant rate of supply of unsupported ^{210}Pb to the sediment. *CATENA* **1978**, *5* (1), 1–8.

(32) Bogdal, C.; Bucheli, T. D.; Agarwal, T.; Anselmetti, F. S.; Blum, F.; Hungerbuehler, K.; Kohler, M.; Schmid, P.; Scheringer, M.; Sobek, A. Contrasting temporal trends and relationships of total organic carbon, black carbon, and polycyclic aromatic hydrocarbons in rural low-altitude and remote high-altitude lakes. *J. Environ. Monit.* **2011**, *13* (5), 1316–1326.

(33) Han, Y.; Cao, J.; Jin, Z.; Liu, S.; An, Z. Comparison of char and soot variations in sediments from lakes Daihai and Taihu. *Quat. Sci.* **2010**, *30* (3), 550–558.

(34) Husain, L.; Khan, A. J.; Ahmed, T.; Swami, K.; Bari, A.; Webber, J. S.; Li, J. Trends in atmospheric elemental carbon concentrations from 1835 to 2005. *J. Geophys. Res.—Atmos.* **2008**, *113* (D13), DOI: 10.1029/2007JD009398.

(35) Muri, G.; Cermelj, B.; Faganeli, J.; Brancelj, A. Black carbon in Slovenian alpine lacustrine sediments. *Chemosphere* **2002**, *46* (8), 1225–1234.

(36) Ming, J.; Xiao, C.; Sun, J.; Kang, S.; Bonasoni, P. Carbonaceous particles in the atmosphere and precipitation of the Nam Co region, central Tibet. *J. Environ. Sci.—China* **2010**, *22* (11), 1748–1756.

(37) Lee, Y. H.; Lamarque, J. F.; Flanner, M. G.; Jiao, C.; Shindell, D. T.; Bernsten, T.; Bisiaux, M. M.; Cao, J.; Collins, W. J.; Curran, M.; Edwards, R.; Faluvegi, G.; Ghan, S.; Horowitz, L. W.; McConnell, J. R.; Myhre, G.; Nagashima, T.; Naik, V.; Rumbold, S. T.; Skeie, R. B.; Sudo, K.; Takemura, T.; Thevenon, F. Evaluation of preindustrial to present-day black carbon and its albedo forcing from ACCMIP (Atmospheric Chemistry and Climate Model Intercomparison Project). *Atmos. Chem. Phys. Discuss.* **2012**, *12* (8), 21713–21778.

(38) Bond, T. C.; Bhardwaj, E.; Dong, R.; Jogani, R.; Jung, S.; Roden, C.; Streets, D. G.; Trautmann, N. M. Historical emissions of black and organic carbon aerosol from energy-related combustion, 1850–2000. *Global Biogeochem. Cycles* **2007**, *21* (2), DOI: 10.1029/2006GB002840.

(39) Chin, M.; Ginoux, P.; Kinne, S.; Torres, O.; Holben, B. N.; Duncan, B. N.; Martin, R. V.; Logan, J. A.; Higurashi, A.; Nakajima, T. Tropospheric aerosol optical thickness from the GOCART model and comparisons with satellite and sun photometer measurements. *J. Atmos. Sci.* **2002**, *59* (3), 461–483.

(40) Chin, M.; Rood, R. B.; Lin, S. J.; Muller, J. F.; Thompson, A. M. Atmospheric sulfur cycle simulated in the global model GOCART—Model description and global properties. *J. Geophys. Res.* **2000**, *105* (D20), 24,671–24,687.

(41) Bond, T. C.; Doherty, S. J.; Fahey, D. W.; Forster, P. M.; Bernsten, T.; DeAngelo, B. J.; Flanner, M. G.; Ghan, S.; Kärcher, B.; Koch, D.; Kinne, S.; Kondo, Y.; Quinn, P. K.; Sarofim, M. C.; Schultz, M. G.; Schulz, M.; Venkataraman, C.; Zhang, H.; Zhang, S.; Bellouin, N.; Guttikunda, S. K.; Hopke, P. K.; Jacobson, M. Z.; Kaiser, J. W.; Klimont, Z.; Lohmann, U.; Schwarz, J. P.; Shindell, D.; Storelvmo, T.; Warren, S. G.; Zender, C. S. Bounding the role of black carbon in the climate system: A scientific assessment. *J. Geophys. Res.—Atmos.* **2013**, DOI: 10.1002/jgrd.50171.

(42) Draxler, R. R.; Rolph, G. D. *HYSPLIT (HYbrid Single-Particle Lagrangian Integrated Trajectory) Model*; NOAA Air Resources Laboratory: Silver Spring, MD, 2003. Available online: <http://www.arl.noaa.gov/ready/hysplit4.html>.

(43) Wang, Y. Q.; Zhang, X. Y.; Draxler, R. R. TrajStat: GIS-based software that uses various trajectory statistical analysis methods to identify potential sources from long-term air pollution measurement data. *Environ. Modell. Software* **2009**, *24* (8), 938–939.

(44) Sahu, S. K.; Beig, G.; Sharma, C. Decadal growth of black carbon emissions in India. *Geophys. Res. Lett.* **2008**, *35* (2), n/a DOI: 10.1029/2007GL032333.

(45) Ramanathan, V.; Ramana, M. V. Persistent, widespread, and strongly absorbing haze over the Himalayan foothills and the Indo-Gangetic Plains. *Pure Appl. Geophys.* **2005**, *162* (8–9), 1609–1626.

(46) Ramanathan, V.; Chung, C.; Kim, D.; Bettge, T.; Buja, L.; Kiehl, J. T.; Washington, W. M.; Fu, Q.; Sikka, D. R.; Wild, M. Atmospheric brown clouds: Impacts on South Asian climate and hydrological cycle. *Proc. Natl. Acad. Sci. U.S.A.* **2005**, *102* (15), 5326–5333.

(47) Bonasoni, P.; Laj, P.; Marinoni, A.; Sprenger, M.; Angelini, F.; Arduini, J.; Bonafé, U.; Calzolari, F.; Colombo, T.; Decesari, S.; Di Biagio, C.; di Sarra, A. G.; Evangelisti, F.; Duchi, R.; Facchini, M. C.; Fuzzi, S.; Gobbi, G. P.; Maione, M.; Panday, A.; Roccatto, F.; Sellegri, E.; Venzac, H.; Verza, G. P.; Villani, P.; Vuilleumoz, E.; Cristofanelli, P. Atmospheric brown clouds in the Himalayas: First two years of continuous observations at the Nepal Climate Observatory-Pyramid (5079 m). *Atmos. Chem. Phys.* **2010**, *10* (15), 7515–7531.

(48) Hindman, E. E.; Upadhyay, B. P. Air pollution transport in the Himalayas of Nepal and Tibet during the 1995–1996 dry season. *Atmos. Environ.* **2002**, *36* (4), 727–739.

(49) Lu, Z.; Streets, D. G.; Zhang, Q.; Wang, S. A novel back-trajectory analysis of the origin of black carbon transported to the Himalayas and Tibetan Plateau during 1996–2010. *Geophys. Res. Lett.* **2012**, *39* (1), L01809 DOI: 10.1029/2011GL049903.

(50) Kopacz, M.; Mauzerall, D. L.; Wang, J.; Leibensperger, E. M.; Henze, D. K.; Singh, K. Origin and radiative forcing of black carbon transported to the Himalayas and Tibetan Plateau. *Atmos. Chem. Phys.* **2011**, *11* (6), 2837–2852.

(51) Han, Y.; Cao, J.; Chow, J. C.; Watson, J. G.; An, Z.; Jin, Z.; Fung, K.; Liu, S. Evaluation of the thermal/optical reflectance method for discrimination between char- and soot-EC. *Chemosphere* **2007**, *69* (4), 569–574.

(52) Han, Y.; Marlon, J.; Cao, J.; Jin, Z.; An, Z. Holocene linkages between char, soot, biomass burning, and climate from Lake Daihai, China. *Global Biogeochem. Cycles* **2012**, *26*, 4.

(53) Gustafsson, Ö.; Kruså, M.; Zencak, Z.; Sheesley, R. J.; Granat, L.; Engström, E.; Praveen, P. S.; Rao, P. S. P.; Leck, C.; Rodhe, H. Brown clouds over South Asia: Biomass or fossil fuel combustion? *Science* **2009**, *323* (5913), 495–498.

(54) Chow, J. C.; Watson, J. G.; Kuhns, H.; Etyemezian, V.; Lowenthal, D. H.; Crow, D.; Kohl, S. D.; Engelbrecht, J. P.; Green, M. C. Source profiles for industrial, mobile, and area sources in the Big Bend Regional Aerosol Visibility and Observational study. *Chemosphere* **2004**, *54* (2), 185–208.

(55) Han, Y.; Cao, J.; Lee, S.; Ho, K.-F.; An, Z. Different characteristics of char and soot in the atmosphere and their ratio as an indicator for source identification in Xi'an, China. *Atmos. Chem. Phys.* **2010**, *10* (2), 595–607.

(56) Sandradewi, J.; Prévôt, A. S. H.; Szidat, S.; Perron, N.; Alfarra, M. R.; Lanz, V. A.; Weingartner, E.; Baltensperger, U. Using Aerosol light absorption measurements for the quantitative determination of

wood burning and traffic emission contributions to particulate matter.

Environ. Sci. Technol. **2008**, *42* (9), 3316–3323.

(57) Carmichael, G. R.; Adhikary, B.; Kulkarni, S.; D’Allura, A.; Tang, Y.; Streets, D.; Zhang, Q.; Bond, T. C.; Ramanathan, V.; Jamroensan, A.; Marrapu, P. Asian aerosols: Current and year 2030 distributions and implications to human health and regional climate change. *Environ. Sci. Technol.* **2009**, *43* (15), 5811–5817.